1 Track-based Algorithms

Standalone track algorithms represent an important part of the Phase-II trigger menu, since they provide the ability to robustly use an independent sub-detector. The tracker is the most granular layer in the CMS L1 decision, so is key for delivering pile-up resilient measurements at L1 which include the primary vertex z-position, track-based jets, and track based missing energy. The harsh pile-up conditions of the Phase-2 LHC make it paramount to seperate L1tracks originating from the primary collision from spurious track hits caused by the large occupancy in the tracking volume. Track purity requirements become a key component to achieve manageable data-recording rates while maintaining low trigger thresholds. This section outlines firmware implemented track based algorithms for reconstructing MET, H_T and clustering tracks into jets.

1.1 Track-based Missing Energy

The vector sum of the transverse momenta (MET) of all particles produced in the primary collision is a key input for BSM triggers at Level-1. For the track-based alogirthm described in this section, one of the main challenges is excluding tracks from bad combinations that give high transverse momentum. Though these tracks are rare in pileup after requiring a tight window around the primary vertex z position, events containing these tracks would dominate an L1 MET trigger. The algorithm makes use of track purity requirements in addition to the $\Delta z\,(PV_z, trk_z)$ requirement to reduce the number of events with poorly measured momentum balance.

The track purity selection is based mainly on the confines of the detector, the track reconstruction algoirthm, and the available track fit quality parameters. The track p_T and η requirements shown in Table 1 are based on the minimal p_T of tracks that can be reconstructed reliably and the tracking acceptance. The minimal number of track layers is also based on the minimal requirement for the track fit. There is a further requirement that 4 of the track layers must also have stubs to remove any 4-stub tracks that were created with only hits in 3 layers. Requirements on the track fit quality measured as $\chi^2_{n.dof}$ is set to a minimum of 50 to reduce tracks that are poorly reconstructed. To further reject high momentum tracks from poorly reconstructed track hit combinations, a new variable, bend consistency, χ^2_{bend} is measured. This measure of the bend of the track is uncorrelated to the $\chi^2_{n.dof}$ from the track fit. χ^2_{bend} is calculated based on the horizontal distance between the two consecutive track hits in a track module, the stubs. The bend consistency quantifys how compatible the bend of the track hits mea-

sured in the detector is compatible with the reconstructed track p_T. The bend consistency variable is defined as:

$$\chi^2_{bend} = \frac{1}{N_{stubs}} \sum_{i=1}^{N_{stubs}} \left(\frac{\beta_i - \beta_i^{exp}}{\sigma_i} \right)^2 \quad (1)$$

where N_{stubs} is the total number of stubs comprising the track, β_i is the measured bend angle for stub i, and β_i^{exp} is the expected bend angle based on the track. A bad combination of track hits tend to have a large value of bend consistency compared to well-reconstructed tracks. The cut on χ^2_{bend} is optimized to lower the fraction of poorly reconstructed tracks that are included in the MET caculation as well as maintaining a reasonable L1 data-rate for a track-based MET trigger.

Track Variable	Cut
N_{stubs} per track layer	≥ 4
p_T	2 GeV
$\chi^2_{n.dof}$	50
χ^2_{bend}	1.75

Table 1: L1 track purity requirements for tracks input to both the MET computation and the L1 track-based jet clustering. Cuts are optimized to preserve a sharp-on turn on in track-based MET, H_T and H_T^{miss} rejecting the bulk of "fake" tracks from bad combination of track hits.

The L1 vertex described in the TSA firmware algorithm in Section **??** is input to the L1 track-based MET algorithm. A window of $\Delta z\,(PV_z, trk_z)$ is required for pseudo-rapidity regions within the tracking acceptance. Table 2 shows the range of values for the allowed range of track-z around around the measured primary vertex z. Central tracks allow for a tight window of 0.4cm while more forward tracks need a wider z-window (as large as 2.2cm) to include tracks within 3σ of the gaussian track z-resolution in the forward regions.

To gauge the performance of track-based MET, we compare the reconstructed track-based MET to simulated tracking particles, which are the simulation level trajectories of charged particles in an event. The tracking particles are used to compute the simulated MET using the same algorithm as the reconstructed L1 tracks. This gives the expected L1 track MET in the case where no fake tracks are included in the MET computation. Figure 1 shows the data-taking L1 rate for the track MET from reconstructed tracks and the tracking particles. Applying only the $|\Delta z\,(PV_z, trk_z)\,|$ cuts in Table 2 gives an L1 rate of 35kHz for a track-based MET threshold at

η range	$\lvert\Delta z\,(PV_z, trk_z)\rvert$ [cm]
$0 \leq \eta < 0.7$	0.4
$0.7 \leq \eta < 1.0$	0.6
$1.0 \leq \eta < 1.2$	0.76
$1.2 \leq \eta < 1.6$	1.0
$1.6 \leq \eta < 2.0$	1.7
$2.0 \leq \eta < 2.4$	2.2

Table 2: Minimum Δz requirements betweeen the primary vertex and track z_0 for each pseudorapidity region for to select tracks for the MET algorithm.

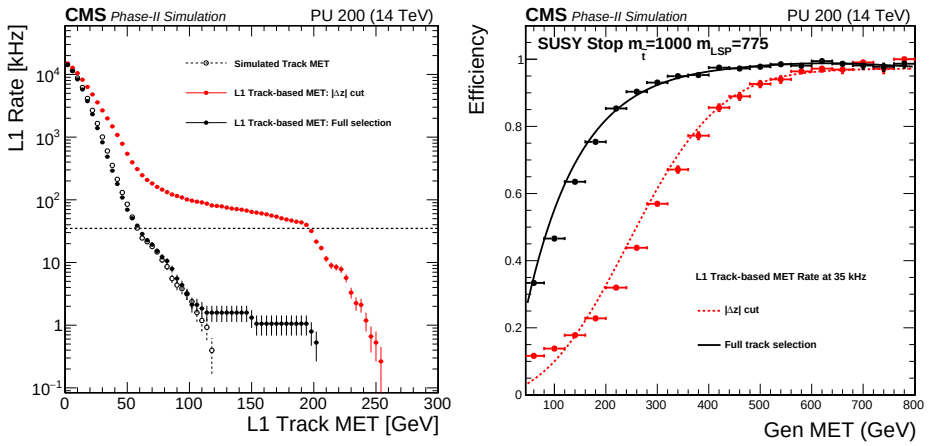

Figure 1:

200GeV. Applying the full track selection inTable 1 shows that this threshold is lowered to 60GeV which is the same threshold as when only simulated true charged particle trajectories are used for the MET computataion. This allows to keep a low trigger turn-on for offline-MET for BSM models like the BSM Stop signal. The trigger turn-on at 95% is lowered from 500 GeV applying only the primary vertex constraint to 300 Gev when including the full selection of track selection.

1.2 Jet Algorithm with Tracks

A rapid firmware implemented track clustering algorithm allows to combine an integrated collection of tracks and output a collection of track-based jets. The track-based jets can then be used for globral trigger quantities like H_T and H_T^{miss}. As described in Section 1.1, the same set of track purity requirements are applied to the input selection of tracks to keep the L1 trigger

objects resilient to pileup. In this section, we describe the simple track clustering alogirthm that is implemented in firmware. Though the algorithm does not make use of an input L1 primary vertex, it can be used as input to the algorithm to make the algorithm more robust against conaminating L1 tracks from pileup.

The clustering of tracks in the η-ϕ plane is done using a nearest-neighbor approach in two 1-dimensional steps. The first phase of the algorithm parses tracks into 27 ϕ regions and 24 η regions, which divides the region of tracking acceptance into cells of that are $\approx 0.2 \times 0.2$. The trk_{z0} is also used to assign the track to a z-cell along the beam spot. The clustering in η-ϕ is done in z-regions that span the beamspot. In between every two z-cells is a third cell to cover the overlapping region and eliminate edge cases where the primary vertex is close to the edge of a given bin. This gives a maximal jet size that is approximately a 3x3 square of cells with a half-side equal to $\Delta R = 0.3$. The width of the z-cell used for this study is 1cm.

Only tracks passing the purity requirements in Table 1 are clustered. In the first layer of track clustering in ϕ, the sum of track p_T, $\sum p_T^{trk}$, in each cell is compared to its two neighbors in ϕ and the p_T is summed into the local maximum cell. The result of this step is to create a list of 1-dimensional track $\sum p_T^{trk}$ clusters based on the local maxima in the ϕ dimension, so that the minimum distance between any two ϕ-clusters is one cell. The next step is to take the ϕ-clusters and check if cells neighbor each other in η, and if they do they are merged into the ϕ-cluster with larger $\sum p_T^{trk}$. The track-based jets are then the list of cells from the local maximum in the η-ϕ plane for a given z-cell. Jets from the primary interaction are found by summing the track-based jet p_T, H_T^{trk}, in each z-cell and taking the jets from the z-bin with the largest H_T^{trk}. In addition, to the $\sum p_T^{trk}$, the track multiplicity is also summed in the same procedure to provide an additional handle for the output collection of track-based jets. This approach gives a list of track-based jet positions in η,ϕ, z_0, p_T, and N_{tracks}.

Figure 2 shows the reconstruction effficiency for this firmware implementable track clustering compared to a full anti-k_T clustering with FASTJET. The same set of input L1 reconstructed tracks is used that pass the track purity requirements. The efficiencies are similar across the range of tracking acceptance and the generator level p_T range, so the approach of 1D nearest neighbor clustering in two steps gives similar efficieny to full 2D jet reconstruction in an algorithm similar to offline jet reconstruction. The largest inefficiency is seen towards the edge of the tracking acceptance $|\eta| > 2.0$ and for lower p_T generator level jets $p_T < 50$GeV which can have lower multiplicity of tracks.

To keep global variables like L1 track-based H_T and H_T^{miss} resilient against

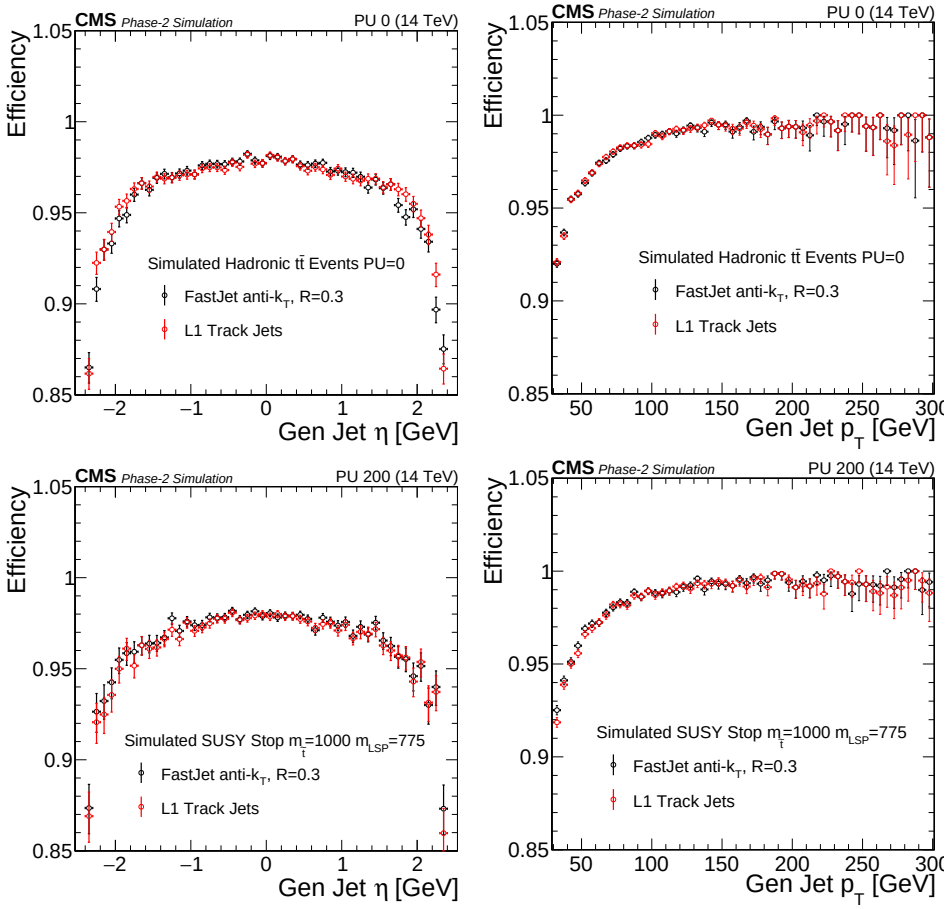

Figure 2: Comparison of the L1 track jet clustering and anti-k_T clustering using FASTJET with $R = 0.3$ with the same input collection of L1 reconstructed tracks. (top) The efficiency in fully hadronic t$\bar{t}$ with no pileup events as a function of generator η(left) and p_T (right). The efficiency is computed by matching the generator-level jet to the reconstructed track jet within $\Delta R < 0.4$.

pileup, we optimize the quality criteria on input L1 tracks to preserve a low trigger threshold while mantaining low data-taking rates. The same criteria as applied for track-based MET is used as in Table 1. When clustering tracks, the track multiplicity in each jet adds an additional handle to reject tracks from bad combinations of track hits which result in fake high p_T tracks. In addition to the input track criteria, jets with $p_T > 50$ are required to have at least 2 tracks and for $p_T > 100$ are required to have at least 3 tracks. Track-based H_T is computed as the scalar sum of p_T for track jets with $p_T > 5$GeV and the 4-vector of the same collection of jets is summed to compute H_T^{miss}.

Figure 3 shows the improvement in both the L1 rate and signal efficiency for the L1 track-based H_T and H_T^{miss} along with the turn-on curves for a BSM stop signal point. The signal model simulates a supersymmetric top decay to its super-partner the top quark and stable lightest supersymmetric particle, $\tilde{\chi}_0^1$. The mass difference between the stop and $\tilde{\chi}_0^1$ is near the top-quark mass so that the missing transverse energy is still small. To measure the trigger turn on a collection of generator level jets is used to emulate offline H_T and H_T^{miss} variables. The generator level collection of jets is made by clustering generator level particles, excluding neutrinos, using the anti-k_T algorithm. The generator level jets considered are those with Gen Jet $p_T > 30$GeV and $|\eta| < 2.4$.

As described in Section 1.1, the rate decreases significantly for missing transverse momentum allowing to trigger on BSM signal events with moderate MET like this BSM stop model. Figure 3 shows the improvement in the L1 data-taking rate, the signal efficiency and the L1 turn-on when reducing the effect of tracks from bad track hit combinations. The improvement is seen for both the he L1 track-based H_T and H_T^{miss} triggers. For a fixed L1 track-based $H_T$rate of 25 kHz, the 95% off-line efficiency turn-on for the stop signal is lowered from 675GeV to 500GeV. The track-based H_T^{miss} trigger lower the threshold from 675GeV down to 310GeV. In both cases, the signal efficiency is greatly increased for a fixed rate to trigger on the BSM stop phase-space with the track purity criteria.

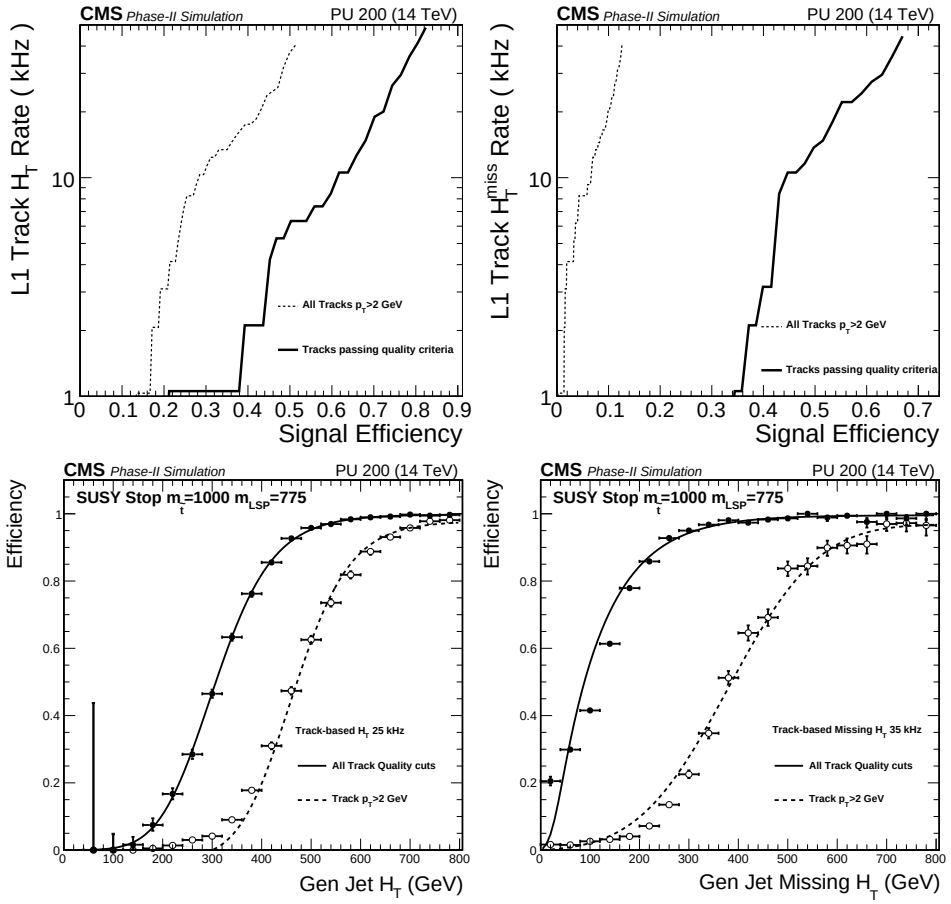

Figure 3: (top) Signal efficiency versus L1 data-taking rates for (left) Track H_T and (right) track H_T^{miss}. The track quality cuts allow to greatly lower these L1 thresholds for a fixed rate by rejecting fake high p_T tracks. (bottom) The trigger-turn on efficiency based on generator level jets to emulate offline selection for the 25kHz L1 threshold for Track H_T(left) and 35kHz L1 threshold for H_T^{miss}(right). The efficiency turn-on for the BSM Stop signal at 95% is greatly lowered with the track purity requirements.